⌘ *Author's Choice*

THE JOURNAL OF BIOLOGICAL CHEMISTRY VOL. 283, NO. 46, pp. 32143–32151, November 14, 2008

Inactive and Active States of the Interferon-inducible Resistance GTPase, Irga6, *in Vivo**[S]

Received for publication, June 25, 2008, and in revised form, September 10, 2008 Published, JBC Papers in Press, September 10, 2008, DOI 10.1074/jbc.M804846200

Natasa Papic[‡], Julia P. Hunn[‡], Nikolaus Pawlowski[‡], Jens Zerrahn[§1], and Jonathan C. Howard[‡2]

From the [‡]Department of Cell Genetics, Institute for Genetics, University of Cologne, 50674 Cologne, Germany and the [§]Department of Immunology, Max-Planck-Institute for Infection Biology, Schumannstrasse 21-22, 10117 Berlin, Germany

Irga6, a myristoylated, interferon-inducible member of the immunity-related GTPase family, contributes to disease resistance against *Toxoplasma gondii* in mice. Accumulation of Irga6 on the *T. gondii* parasitophorous vacuole membrane is associated with vesiculation and ultimately disruption of the vacuolar membrane in a process that requires an intact GTP-binding domain. The role of the GTP-binding domain of Irga6 in pathogen resistance is, however, unclear. We provide evidence that Irga6 in interferon-induced, uninfected cells is predominantly in a GDP-bound state that is maintained by other interferon-induced proteins. However, Irga6 that accumulates on the parasitophorous vacuole membrane after Toxoplasma infection is in the GTP-bound form. We demonstrate that a monoclonal antibody, 10D7, specifically detects GTP-bound Irga6, and we show that the formation of the 10D7 epitope follows from a GTP-dependent conformational transition of the N terminus of Irga6, anticipating an important role of the myristoyl group on Irga6 function *in vivo*.

The biological activity of GTPases depends on the control of the GTP binding and hydrolysis cycle. For several classes of GTPase, such as the Ras family of small GTPases, the G-proteins coupled to seven-transmembrane receptors, and the translation initiation and elongation factors, the molecular mechanisms by which the GTP cycle is controlled are known in considerable detail, and the biological contexts in which the activity cycles of the proteins function are well understood. All of these proteins function in cyclical processes in cells where the binding of GTP by a GTPase initiates a conformational change that drives a forward step in the cycle, whereas the hydrolysis of GTP to GDP terminates the forward activity and reverts the GTPase to its inactive ground state. There has been considerable recent interest in the function of several anomalous large GTPase families active in cell-autonomous immune resistance. However, no systematic study of the role of the GTP binding and hydrolysis cycle has been undertaken in order to define the functions of these proteins in biological processes associated with active pathogen resistance. In this paper, we have made some progress toward defining components of the activity cycle *in vivo* of Irga6, an interferon-inducible 47-kDa GTPase of the IRG family in mice.

IRG[3] proteins are 47-kDa, interferon-inducible GTPases intimately involved in disease resistance against intracellular parasites in mice (1–12). Some biochemical parameters and the crystal structure of one member of the family, Irga6 (formerly IIGP1), have been determined (13). Irga6 possesses a Ras-like GTP-binding domain slung between two helical modules of unknown function. The N terminus carries a myristoylation signal (14) that is active *in vivo* (15). The nonmyristoylated protein purified from *Escherichia coli* has affinities in the micromolar range for GDP (~1 μM) and for GTP (~15 μM) and a low basal turnover rate from GTP to GDP of less than 0.1/min (16). Like many anomalous large GTPases, Irga6 shows cooperativity in specific turnover rate, with a maximum of ~2.0/min. Cooperativity of Irga6 is also reflected in a tendency to form oligomers *in vitro* upon the addition of GTP that resolve upon hydrolysis of the substrate (16).

The mode of action of IRG proteins *in vivo* is not well understood. After induction by interferons, IRG proteins including Irga6 are expressed at high levels in all cell types analyzed (17). Irga6 is ~60% associated with the ER membrane and 40% freely cytosolic (15). Within a few minutes after infection by the protozoan parasite, *Toxoplasma gondii*, cytoplasmic Irga6 accumulates on the membrane of the parasitophorous vacuole (PVM) (8).[4] Within 1–2 h, the PVM becomes vesiculated and ultimately disrupts, the parasite is exposed to the cytosol, and parasite replication is interrupted (6, 8). This succession of events is blocked if an interferon-stimulated infected cell is also expressing what we have previously described as a "functionally dominant negative" mutant of Irga6, Irga6-K82A, demonstrating that the cell-autonomous resistance process is dependent on the function of IRG proteins and suggesting the importance of GTP binding and hydrolysis in the biological function (8).

Next to nothing is known about the role of the GTPase function of the IRG proteins in pathogen resistance. In an early

* This study was supported by Deutsche Forschungsgemeinschaft Grants SPP1110, SFB635, and SFB670 and by the University of Cologne. The costs of publication of this article were defrayed in part by the payment of page charges. This article must therefore be hereby marked "*advertisement*" in accordance with 18 U.S.C. Section 1734 solely to indicate this fact.

[S] The on-line version of this article (available at http://www.jbc.org) contains supplemental Fig. 1.

⌘ *Author's Choice*—Final version full access.

[1] Present address: Institute of Clinical Pharmacology PAREXEL International GmbH, 14050 Berlin, Germany.

[2] To whom correspondence should be addressed: Institute for Genetics, University of Cologne, Zülpicher Str. 47, 50674 Cologne, Germany. Tel.: 49-2214704864; Fax: 49-2214706749; E-mail: j.howard@uni-koeln.de.

[3] The abbreviations used are: IRG, immunity-related GTPase; IMDM, Iscove's modified Dulbecco's medium; AlFx, aluminum fluoride complex; GTPγS, guanosine 5′-(3-*O*-thio)triphosphate; PVM, parasitophorous vacuole membrane; IFNγ, interferon γ; PBS, phosphate-buffered saline; ER, endoplasmic reticulum.

[4] A. Khaminets, unpublished data.

experiment, evidence was presented that another IRG protein, Irgm3 (formerly IGTP), isolated by immunoprecipitation from interferon-stimulated cells, co-purified with bound GTP, and the authors suggested that, unusually for a GTPase, Irgm3 exists in interferon-induced cells constitutively in the GTP-bound state (18). It has so far not proved possible to effect a biochemical purification of Irgm3, so the kinetic parameters of this member of the IRG family, either as a guanylate binding protein or as a GTPase, are not known.

In this report, we have begun an analysis of the nucleotide-bound state of Irga6 *in vivo* in uninfected and infected cells. Our experiments strongly suggest that the resting state of Irga6 in the IFN-induced but uninfected cell is GDP-bound, whereas the Irga6 that accumulates on the PVM after *T. gondii* infection is in the GTP-bound state. Furthermore, our data suggest that the GDP-bound state of Irga6 in uninfected cells is actively maintained by a further interferon-inducible protein or proteins. We have shown elsewhere that this regulation is an active property of certain IRG proteins themselves (19). These results thus suggest that the resistance properties of Irga6 will prove to be properties of the GTP-bound, active state of the protein at the parasitophorous vacuole membrane. During the course of these studies, we demonstrated that a monoclonal antibody can detect the GTP-bound state of Irga6 with high specificity, and we show that the target epitope of this reagent is subject to conformational influences both from local structural elements and distantly from the nucleotide binding site.

EXPERIMENTAL PROCEDURES

Expression Constructs—The pGW1H-Irga6cTag1 construct was generated by amplification of the Irga6cTag1 sequence from pGEX-4T-2-Irga6cTag1 (former pGEX-4T-2-IIGP-m) (16) by using Irga6cTag1 forward (5′-ccccccccgtcgaccaccatgggtcagctgttctcttcacctaag-3′) and reverse (5′-ccccccccgtcgactcagtcacgatgcggccgctcgagtcggcctag-3′) primers and cloned into pGW1H vector (British Biotech) by SalI digestion. Mutations were introduced into the coding region of pGW1H-Irga6wt (15), pGW1H-Irga6cTag1, and pGEX-4T2-Irga6wt (16) according to the QuikChange site-directed mutagenesis kit (Stratagene) using the following forward and corresponding reverse primers: G2A, 5′-gagtcgaccaccatggctcagctgttctcttca-3′; Δ7–12, 5′-gggtcagctgttctctaataatgatttgccc-3′; Δ7–25, 5′-ccaccatgggtcagctgttctctaaatttaatacggg-3′; Δ20–25, 5′-gaataatgatttgccctccagcaaatttaatacgggaag-3′; F20A, 5′-gagaataatgatttgccctccagcgctactggttatttaag-3′; T21A, 5′-gaataatgatttgccctccagctttgctggttatttaag-3′; G22A, 5′-gccctccagctttactgcttattttaagaaatttaatacggg-3′; Y23A, 5′-gccctccagctttactggtgcttttaagaaatttaatacggg-3′; F24A, 5′-gccctccagctttactggttatgctaagaaatttaatacgggaag-3′; K25A, 5′-gccctccagctttactggttattttgcgaaatttaatacgggaag-3′; K82A, 5′-gggagacgggatcaggggcgtccagcttcatcaataccc-3′; S83N, 5′-ggagacgggatcagggaagaacagcttcatcaataccctg-3′; E106A, 5′-gctaaaactggggtggtggcggtaaccatggaaag-3′.

Cell Culture and Serological Reagents—L929 (CCL-1) and gs3T3 (Invitrogen) mouse fibroblasts were cultured in IMDM or Dulbecco's modified Eagle's medium (both GIBCO) supplemented with 10% fetal calf serum (Biochrom). Hybridoma 10D7 and 10E7 cells were grown in IMDM, supplemented with 5% fetal calf serum. Cells were induced with 200 units/ml IFNγ (Cell Concepts) for 24 h and transfected using FUGENE6 transfection reagent according to the manufacturer's protocol (Roche Applied Science). Propagation of *T. gondii* strain ME49 was done as described previously (8). gs3T3 cells were infected for 2 h with *T. gondii* ME49 strain at a multiplicity of infection of 8 24 h after IFNγ stimulation. The following serological reagents were used: anti-Irga6 mouse monoclonal antibodies 10D7 and 10E7, anti-Irga6 rabbit polyclonal serum 165, anti-cTag1 rabbit polyclonal serum 2600 (8), donkey-anti-mouse Alexa 546, donkey anti-rabbit Alexa 488 (all from Molecular Probes), goat anti-mouse κ light chain (Bethyl), goat anti-mouse κ light chain horseradish peroxidase (Bethyl), goat anti-mouse κ light chain-fluorescein isothiocyanate (Southern Biotech), 4′,6-diamidino-2-phenylindole (Roche Applied Science), and donkey anti-rabbit, donkey anti-goat, and goat anti-mouse horseradish peroxidase (all from Amersham Biosciences).

Antibody Purification and Papain Digestion—10D7 and 10E7 antibodies were purified from corresponding hybridoma supernatants over a Protein A-Sepharose column (Amersham Biosciences). Antibody was eluted with 50 mM sodium acetate, pH 3.5, 150 mM NaCl and pH-neutralized to 7.5 with 1 M Tris, pH 11. Buffer was exchanged five times subsequently by dilution of antibody-containing sample in papain buffer (75 mM phosphate buffer, pH 7.0, 75 mM NaCl, 2 mM EDTA) and concentrated in a centrifugal concentrator (Vivaspin20; Sartorius) with a 10 kDa cut-off filter at 2000 × *g* at 4 °C. The concentration of the antibodies was determined by using formula, concentration of antibody (mg/ml) = $0.8 \times A_{280}$. Papain digestion was done according to Ref. 20. The papain-digested antibodies were further purified on a HiLoad 26/60 Superdex 75 preparation grade column (Amersham Biosciences) in papain buffer. Samples were incubated in SDS-PAGE sample buffer under nonreducing conditions and subjected to SDS-PAGE. Proteins were detected by colloidal Coomassie staining.

Treatment with Aluminum Fluoride—$AlCl_3$ (Sigma) was added to 10 ml of IMDM containing no fetal calf serum to a final concentration of 300 μM and mixed by vigorous shaking. Subsequently, NaF (Sigma) was added to a final concentration of 10 mM and mixed, and the final solution was applied to confluent L929 cells previously induced with IFNγ or transfected for 24 h. Cells were incubated in aluminum fluoride complex (AlFx) solution for 30 min at 37 °C and then washed with cold PBS and collected by scraping. Cell pellets were lysed in 0.1% Thesit/PBS containing 300 μM $AlCl_3$ and 10 mM NaF in the presence or absence of 0.5 mM GTP for 1 h at 4 °C.

Immunoprecipitation and Immunofluorescence—Immunoprecipitation was modified from Ref. 21. 1×10^6 L929 fibroblasts/sample were induced with IFNγ and/or transfected for 24 h (or left untreated) and harvested by scraping. Cells were lysed in 0.1% Thesit, 3 mM $MgCl_2$, PBS, Complete Mini protease inhibitor mixture without EDTA (Roche Applied Science) for 1 h at 4 °C in the absence of nucleotide or in the presence of 0.5 mM GDP, GTP, GTPγS, or 300 μM $AlCl_3$ and 10 mM NaF in the presence or absence of 0.5 mM GTP (all from Sigma). Protein A-Sepharose™ CL-4B beads (Amersham Biosciences) were incubated with 10D7 monoclonal mouse anti-Irga6 antibody or 2600 (anti-cTag1) polyclonal rabbit serum for 1 h at 4 °C. Bound proteins were eluted by boiling for 10 min in elution buffer (100 mM

Tris/HCl, pH 8.5, 0.5% SDS) with SDS-PAGE sample buffer (50 mM Tris/HCl, pH 6.1, 1% SDS, 5% glycerol, 0.0025% bromphenol blue (w/v), 0.7% β-mercaptoethanol). Immunofluorescence was preformed as previously described (15).

Colloidal Coomassie Staining—Gels were washed 30 min with H_2O and subsequently placed in incubation solution (17% ammonium sulfate (w/v), 20% MeOH, 2% phosphoric acid). After a 60-min incubation, solid Coomassie Brilliant Blue G-250 (Serva) was added to the solution to a concentration of 330 mg/500 ml and incubated 1–2 days. The gels were destained by incubation in 20% MeOH for 1 min and stored in 5% acetic acid. All was done at room temperature and while shaking.

Expression and Purification of Irga6 Proteins from E. coli—pGEX-4T-2-Irga6 constructs were transformed into BL-21 *E. coli* strain. Cells were grown at 37 °C to an A_{600} of 0.8 when the expression of glutathione *S*-transferase-fused Irga6 proteins was induced by 0.1 mM isopropyl-β-D-thiogalactoside at 18 °C overnight. Cells were harvested (5000 × *g*, 15 min, 4 °C); resuspended in PBS, 2 mM DTT, Complete Mini protease inhibitor mixture without EDTA (Roche Applied Science) and lysed using a microfluidizer (EmulsiFlex-C5; Avestin) at a pressure of 150 megapascals. The lysates were cleared by centrifugation at 50,000 × *g* for 60 min at 4 °C. The soluble fraction was purified on a glutathione-Sepharose affinity column (GSTrap FF 5 ml; Amersham Biosciences) equilibrated with PBS, 2 mM dithiothreitol. The glutathione *S*-transferase domain was cleaved off by overnight incubation with thrombin (20 units/ml; Serva) on the resin at 4 °C. Free Irga6 was eluted with PBS, 2 mM dithiothreitol, and the protein content in fractions was analyzed by SDS-PAGE and visualized by Coomassie staining (22). The protein-containing fractions were concentrated in a centrifugal concentrator (Vivaspin20; Sartorius). Aliquots were shock-frozen in liquid nitrogen and stored at −80 °C. The concentration of protein was determined by UV spectrophotometry at 280 nm.

RESULTS

The Anti-Irga6 Monoclonal Antibody, 10D7, Recognizes a Distinct Conformation of Irga6 Present at the T. gondii PVM—Irga6 is detected in a reticular pattern throughout IFNγ-induced cells, most accurately co-localizing with the ER marker TAP (15). Upon infection with *T. gondii*, however, Irga6 is rapidly recruited to the PVM (8). In IFNγ-induced mouse fibroblasts, we compared by indirect immunofluorescence the intracellular binding behavior of two IgG1 monoclonal antibodies raised against recombinant Irga6. Antibody 10E7 showed strong fine reticular staining typical of ER-localized IFNγ-induced Irga6 (15), whereas cytoplasmic Irga6 was scarcely detectable with antibody 10D7 (Fig. 1). In contrast, 10D7 and 10E7 gave equally strong signals for Irga6 on the PVM of infecting *T. gondii* organisms (Fig. 1, *arrowheads*). We sought to distinguish between two alternative explanations for these results. Either 10D7 specifically recognized a determinant exposed only on the Irga6 bound to the PVM, or 10D7 was a low affinity antibody that could bind bivalently and hence stably to the concentrated, immobilized Irga6 at the PVM but not to the distributed Irga6 in the cytoplasmic pool. We therefore prepared monovalent Fab fragments of 10D7 by papain digestion. Since

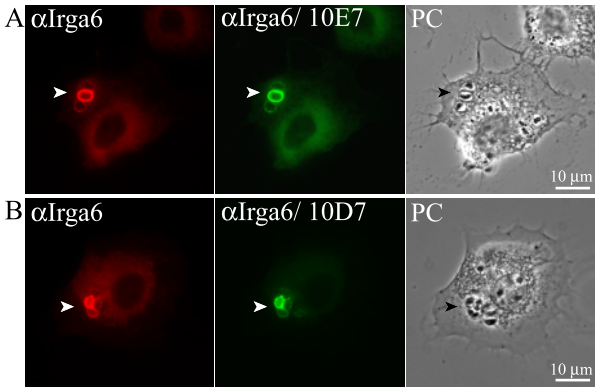

FIGURE 1. **10D7 antibody detects Irga6 at the PVM but not at the ER.** gs3T3 fibroblasts were induced with IFNγ for 24 h prior to 2-h infection with *T. gondii* ME49 strain with a multiplicity of infection of 8. Irga6 protein was labeled with rabbit anti-Irga6 polyclonal serum 165 (*red*) and with mouse monoclonal anti-Irga6 antibodies 10E7 (*A*) or 10D7 (*B*) (*green*). *PC*, phase-contrast images. Parasitophorous vacuoles are indicated by the *arrowheads*. 10D7 detected Irga6 on the PVM efficiently but the cytoplasmic, ER membrane-associated Irga6 at a barely detectable level.

monovalent Fab fragments are unable to bind bivalently, they should bind equally, whether weakly or strongly, to distributed and aggregated targets. Following papain digestion, monovalent fragments were separated from residual bivalent material by size exclusion chromatography (Fig. 2, *A* and *B*, and supplemental Fig. 1). The binding activities of two fractions (B8 and B15, apparent molecular weights of 55,000 and 45,000, respectively) were compared by dilution in a Western blot against bacterially purified Irga6 protein (Fig. 2*C*). The titer of the later eluting fraction (B15) was higher than that of the earlier eluting fraction (B8), showing that the activity detected was not derived from trailing of residual bivalent material down the column. This result already indicated that monovalent 10D7 Fab fragment (fraction B15) has an affinity for Irga6 on a Western blot comparable with that of the native 10D7. It did not, however, prove that the monovalent affinity of 10D7 for Irga6 at the PVM is also high. We therefore examined the binding of Fab fragments from 10D7 to Irga6 accumulated on the *T. gondii* PVM in interferon-induced cells. The fragments were detected with a fluorescent conjugate of an anti-mouse κ light chain second stage reagent and the intensities of 10D7 Fab and the bivalent native 10D7 antibody signals examined at constant exposure times. Fig. 2*D* shows that strong signals were detected at the PVM from both 10D7 Fab and intact 10D7, and the exposure times required for equivalent signal strength were essentially identical. Thus, 10D7 binds with high affinity to Irga6 at the PVM because Irga6 in this site adopts a conformation distinct from that present in the distributed cytoplasmic pool. Subsequent experiments were dedicated to showing that the two distinct *in vivo* conformations represent GTP-bound and GDP-bound states, respectively.

The Formation of Irga6 Oligomers in Vivo—Since purified Irga6 forms enzymatically active oligomers *in vitro* in the presence of GTP (16), we were interested to find out whether such oligomers could be detected in the uninfected, interferon-induced cell. To this end, we transfected IFNγ-induced fibroblasts expressing wild-type Irga6 with an Irga6 construct modified at the C terminus with an 11-residue peptide tag, cTag1

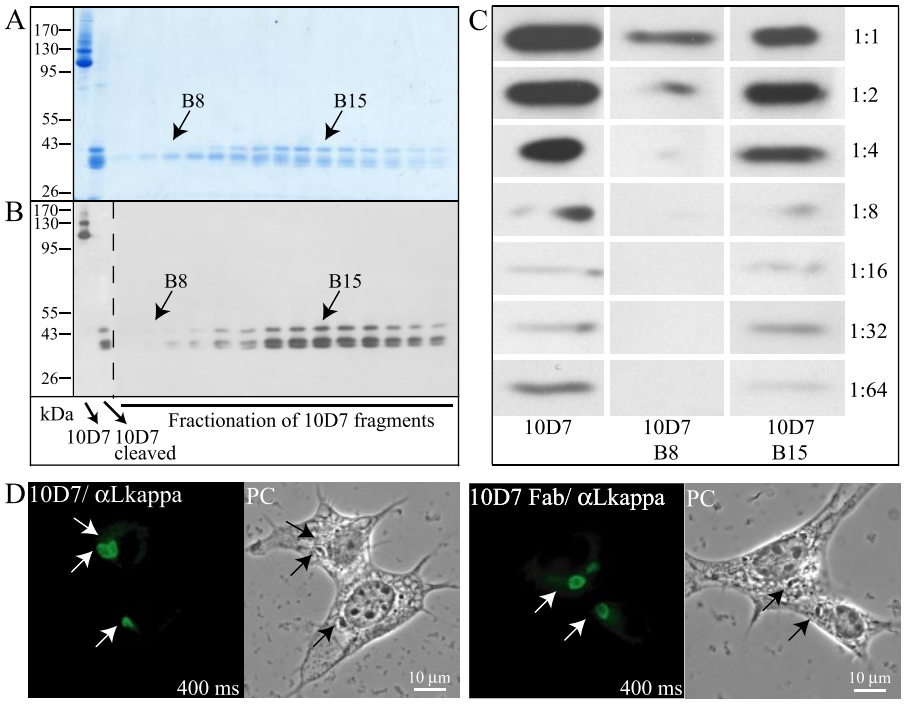

FIGURE 2. **10D7 is a high affinity antibody.** Papain-cleaved 10D7 antibody was separated on a Superdex 75 column. Fractions were subjected to SDS-PAGE on 7.5% gels under nonreducing conditions, and protein was detected by colloidal Coomassie staining (*A*) or Western blot (*B*) using goat anti-mouse κ light chain and donkey anti-goat horseradish peroxidase antibodies as primary and secondary stage detection reagents, respectively. The apparent molecular weight of native 10D7 IgG on SDS-PAGE was dependent on gel conditions. In relatively short runs in 7.5% gels, 10D7 ran in a complex band pattern below 130 kDa (*A* and *B*). However, the same material run longer in a 10% gel behaved rather normally, reaching an average position at or even above 150 kDa (see supplemental Fig. 1). Papain-cleaved fragments were shown to have an apparent molecular mass of ~40 kDa in the 7.5% gel system (*A* and *B*). *C*, relative affinity of putative Fab fractions B8 and B15 of papain-cleaved 10D7 was estimated by binding to recombinant Irga6 fixed to the nitrocellulose membrane. 10 μg/ml antibodies was considered as 1:1 and further dilutions were made, 1:2, 1:4, 1:8, 1:16, 1:32, and 1:64. A similar dilution series of uncleaved native 10D7 was made as positive controls. Detection of 10D7 and 10D7 fragments was done as in *B*. Monovalent 10D7 Fab fragment (fraction B15) has an affinity for denatured Irga6 on a Western blot comparable with that of the native 10D7. *D*, gs3T3 fibroblasts were induced with IFNγ 24 h followed by infection with *T. gondii* ME49 strain for 2 h. Irga6 was detected with 10 μg/ml of 10D7 antibody (10D7) or 10D7 Fab; as secondary detection reagent, goat anti-mouse κ light chain-fluorescein isothiocyanate (α*Lkappa*) was used. This secondary reagent detects papain-cleaved Fab and intact 10D7 with the same efficiency. The *arrows* indicate positions of *T. gondii* vacuoles. *PC*, phase-contrast images.

(see "Experimental Procedures"), which causes a detectable size shift in SDS-PAGE. Twenty-four hours after transfection and interferon induction, Irga6cTag1 was immunoprecipitated from detergent lysates of the cells, and the product was resolved on SDS-PAGE and analyzed by Western blot for Irga6 (Fig. 3*A*). In the absence of added nucleotides, no co-precipitated wild-type Irga6 could be detected (*lane 1*); thus, there is no stable Irga6-Irga6 association in IFNγ-induced cells. The addition of GDP or GTP to the lysate also failed to permit detectable co-precipitation of native Irga6 (*lanes 2* and *3*), but in the presence of the nonhydrolyzable GTP analog, GTPγS (*lane 6*), native Irga6 was strongly co-precipitated. These results suggested the possibility that Irga6cTag1 may indeed occur in cells in GTP-dependent oligomers with native Irga6 but that these rapidly hydrolyze GTP and dissociate again. However, the addition of nucleotides to the lysis risks the formation of artifactual postlysis oligomerization, and the results may not reflect the situation in the cell before lysis. It was shown earlier that the addition of AlFx and GTP to bacterially purified Irga6 *in vitro* resulted in the formation of irreversibly locked oligomers (16). The affinity of Irga6 for GDP is not altered by the presence of AlFx,[5] and the addition of GDP and AlFx to Irga6 does not cause oligomerization. Thus, the AlFx binding site is accessible only during the catalytic step immediately after cleavage of the γ-phosphate from GTP. AlFx is cell-permeant and therefore able to trap active Irga6 complexes *in vivo*. Although the addition of both AlFx and GTP during the immunoprecipitation procedure resulted in the co-precipitation of a significant amount of native Irga6 (*lane 5*), preincubation of the cells in AlFx before lysis failed to trap any mixed oligomers containing native Irga6 (*lane 4*). This result suggested, first, that no active, GTP-dependent oligomers are present in the uninfected, interferon-induced cells, and, second, that the complexes that were co-precipitated following the addition of nucleotides and AlFx to the lysate may have been formed postlysis. Proof that all of the mixed oligomers detected in Fig. 3*A* were indeed formed postlysis during the immunoprecipitation procedure itself was provided by the results of the experiment shown in Fig. 3*C*. Two separate cell populations were mixed at the time of lysis, one interferon-induced and the other transfected with Irga6cTag1. The mixed lysate was then immunoprecipitated for Irga6cTag1 in the presence of various nucleotides and AlFx (Fig. 3*C*, (*i*) + (*t*)) and compared with similar immunoprecipitates from the lysate of a single cell population that was both IFNγ-induced and transfected with Irga6cTag1 (Fig. 3*C*, (*i* + *t*)). Fig. 3*C* shows that the addition of GTPγS or GTP + AlFx (*lanes 5* and *6*) to the mixed lysates ((*i*) + (*t*)) resulted in strong co-precipitation of the native Irga6, quantitatively equivalent to the co-precipitates found in transfected and IFNγ-induced ((*i* + *t*)) cells. In summary, the results shown in Fig. 3, *A* and *C*, taken together provide strong evidence that Irga6 expressed in IFNγ-induced cells is not present in the form of GTP-dependent oligomers of any size, including dimers.

We have reported that Irga6 is substantially mislocalized when expressed in cells that have not been induced with IFNγ (15, 19). The mislocalization is seen as small cytoplasmic aggregates instead of the smooth ER-related localization seen in IFNγ-induced cells, and it can be prevented if the transfected

[5] R. Uthaiah, unpublished results.

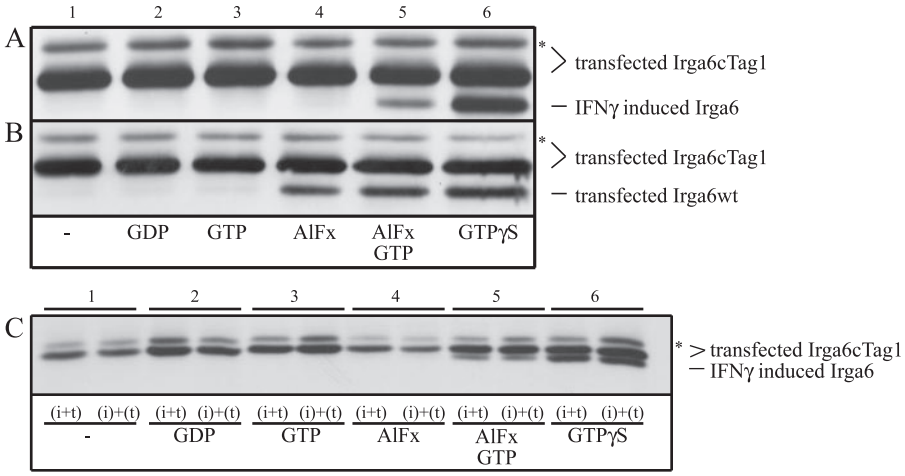

FIGURE 3. **In uninfected cells, Irga6 forms GTP-dependent oligomers only in the absence of IFNγ.** L929 fibroblasts were simultaneously induced with IFNγ and transfected with Irga6cTag1 24 h before lysis (*A*), not induced with IFNγ but simultaneously transfected with both Irga6wt and Irga6cTag1 24 h before lysis (*B*), or either simultaneously ((*i* + *t*)) or separately ((*i*) + (*t*)) induced with IFNγ and transfected with Irga6cTag1 24 h before lysis (*C*). Irga6 was immunoprecipitated from lysates with rabbit anti-cTag1 serum. Cells were either preincubated with AlFx and subsequently lysed in the absence of nucleotides (*lane 4*) or without preincubation lysed in the presence of nucleotides with or without AlFx (*lanes 2*, *3*, *5*, and *6*). Cells in *lane 1* were immunoprecipitated without preincubation and without additives during the immunoprecipitation. Irga6 proteins in immunoprecipitates were detected with 10D7 antibody in a Western blot. A second band above wild-type Irga6cTag1 (marked with a *single asterisk*) is always found in Western blots of transfected Irga6; the nature of this presumed modification is unknown.

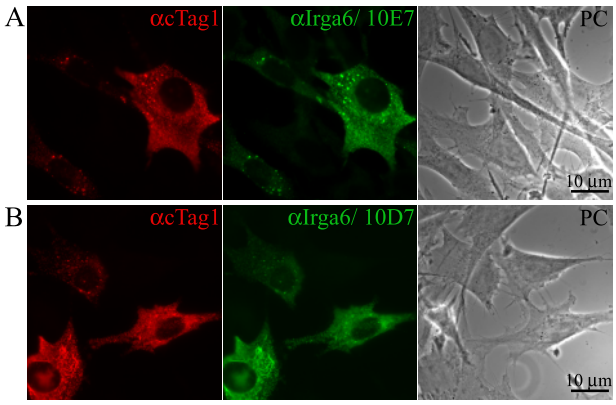

FIGURE 4. **In noninduced cells, 10D7 detects aggregated Irga6 as efficiently as 10E7 antibody.** Untreated gs3T3 fibroblasts were transfected with Irga6cTag1 and stained 24 h later with anti-cTag1 polyclonal serum (*red*) and with either 10E7 (*A*) or 10D7 (*B*) monoclonal antibodies (*green*). *PC*, phase-contrast images.

cells are also induced with IFNγ (19). The possibility that these aggregates represented GTP-dependent oligomers was tested directly by co-immunoprecipitation from uninduced cells transfected simultaneously with both native Irga6 and Irga6cTag1 (Fig. 3*B*). In this case, unlike in IFNγ-induced cells (Fig. 3*A*), preincubation of the cells with AlFx (*lane 4*), before detergent lysis and in the absence of any exogenous nucleotide, allowed strong subsequent co-precipitation of wild-type Irga6 with Irga6cTag1. Since the AlFx binding site is inaccessible on GDP-bound Irga6, these results show that in the absence of other IFNγ-induced proteins intracellular Irga6 exists at least partially in hydrolytically active, GTP-containing oligomers, which can be stabilized by AlFx in the living cell. These experiments showed that Irga6 can exist in two alternative states *in vivo*, namely monodispersed hydrolytically inert in the IFN-induced cell or assembled in GTP-dependent hydrolytically active oligomers in the transfected, uninduced cell.

The Conformation-sensitive Monoclonal Antibody, 10D7, Binds Irga6 in the GTP-bound Form—Since 10D7 binds very inefficiently to the monodispersed, cytoplasmic form of Irga6 expressed in IFNγ-induced cells, it was of interest to find out whether the GTP-dependent Irga6 aggregates forming in transfected cells are recognized by 10D7. Figs. 4 and 5*A* show that 10D7 indeed binds as strongly to Irga6 aggregates in transfected cells as does the indiscriminate monoclonal antibody, 10E7 (Fig. 4), or the anti-cTag1-specific serum 2600 (Fig. 5*A*). Thus, the Irga6 conformation recognized by 10D7 is the GTP-dependent, hydrolytically active conformation, implying that Irga6 detected by 10D7 around the PVM in IFN-induced cells is itself in the GTP-bound state. The binding of 10D7 to transfected Irga6 was largely eliminated if transfected cells were simultaneously induced with IFNγ, especially in cells expressing relatively little of the transfected protein (Fig. 5*B*, *arrow*). This result is consistent with other evidence that the presence of other IFNγ-induced IRG proteins normally maintains Irga6 in the inactive state (19).

That 10D7 binds specifically to the GTP-bound, active state of Irga6 *in vivo* was further supported by the behavior of two nucleotide-binding site mutants of Irga6, the "functionally dominant negative" P-loop mutant, Irga6-K82A, and a further mutant that has lost affinity for both GDP and GTP, Irga6-S83N (19). We have shown elsewhere that transfected Irga6-K82A is functionally dominant negative *in vivo*, co-localizing in smaller or larger cytoplasmic aggregates with IFNγ-induced wild-type Irga6 and inhibiting the accumulation of the latter on the PVM of infecting Toxoplasma (8, 19). We have further shown that, although behaving functionally as a dominant negative, Irga6-K82A binds GTP with wild-type affinity but fails to hydrolyze it (19). Consistent with the suggestion that 10D7 binds to the GTP-bound active form of Irga6, 10D7 also bound strongly to Irga6 in cells transfected with Irga6-K82A, whether they were IFNγ-induced (Fig. 5*C*) or not (Fig. 5*D*), while binding weakly to cells transfected with Irga6-S83N, again independent of simultaneous IFNγ induction (Fig. 5, *E* and *F*).

The Nature of the 10D7 Epitope and Conditions for Its Formation—The 10D7 epitope of Irga6 was constitutively exposed on Western blots (Fig. 2*C*), suggesting that it is a linear epitope expressed by denatured protein. We further observed that the 10D7 epitope was also constitutively accessible in cells expressing the N-terminal 69 residues of Irga6 tagged at the C terminus with green fluorescent protein (data not shown). Thus, expression of the epitope is not dependent on the pres-

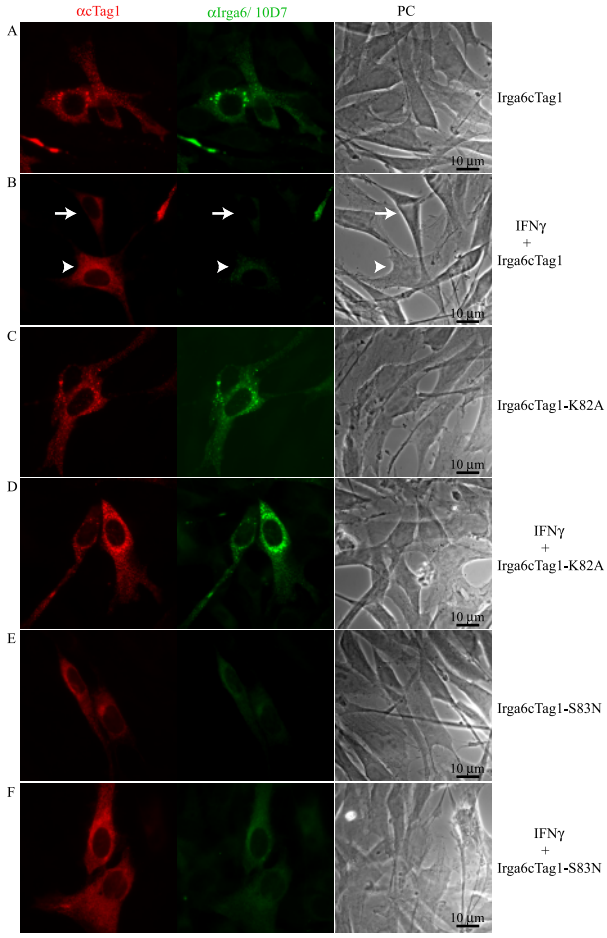

FIGURE 5. **Hydrolysis-deficient dominant-negative mutant of Irga6 forms aggregates independently of IFNγ-induced factors and constitutively exposes the 10D7 epitope.** Irga6cTag1-wt (*A* and *B*), Irga6cTag1-K82A (*C* and *D*; functionally dominant negative), and Irga6cTag1-S83N (*E* and *F*) constructs were transfected into gs3T3 fibroblasts either in the absence (*A*, *C*, and *E*) or in the presence of IFNγ induction (*B*, *D*, and *F*). Transfected cells were stained 24 h later with 10D7 antibody (*green*) and anti-cTag1 serum (*red*). Images were taken with the same exposure time. The *arrow* and *arrowhead* in *B* indicate cells with lower and higher levels of transfected Irga6cTag1 protein, respectively. Treatment with IFNγ markedly attenuates the 10D7 signal on transfected wild-type Irga6cTag1 (*B*) but has no impact on the 10D7 signal of transfected Irga6cTag1-K82A (*C* and *D*). The 10D7 signal is weak on Irga6cTag1-S83N independently of IFNγ treatment (*E* and *F*). *PC*, phase-contrast images.

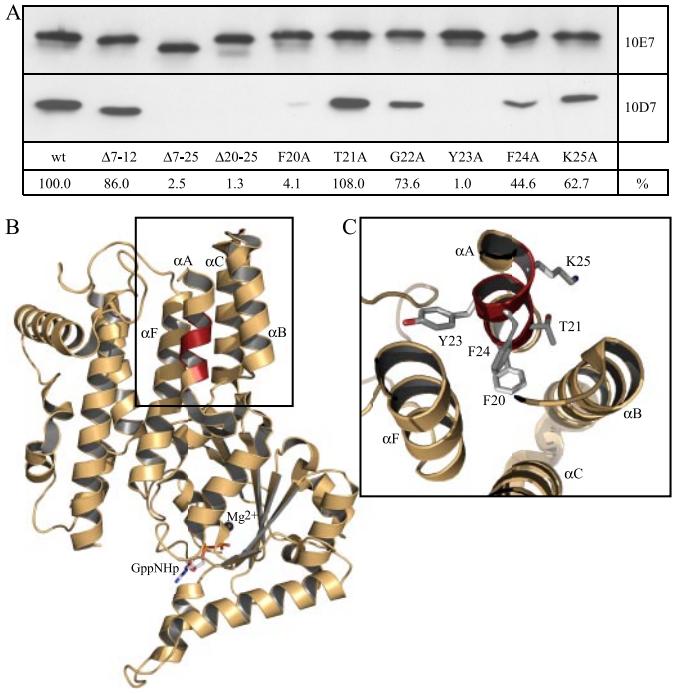

FIGURE 6. **10D7 epitope is located in the Helix A of Irga6 protein.** *A*, purified, nonmyristoylated recombinant Irga6wt, -Δ7–12, -Δ7–25, -Δ20–25, -F20A, -T21A, -G22A, -Y23A, -F24A, and -K25A proteins were subjected to SDS-PAGE and detected in Western blot with 10E7 and 10D7 antibodies. 10D7 signals were quantified, and values for mutants are given as percentages relative to the Irga6wt signal; *B*, crystal structure of Irga6 monomer (13), with Helix A, containing the 10D7 epitope, amino acids 20–25, indicated in *red*. The myristoyl group and the first 12 N-terminal amino acids have not yet been crystallographically resolved. GppNHp and Mg^{2+} are shown as an atomic *stick figure* and *black sphere*, respectively; *C*, *enlarged view* of the structure shown in Fig. 6*B*, looking from *below* on the 4-helix bundle of which Helix A is a member. The orientations of the side chains of Phe^{20}, Thr^{21}, Tyr^{23}, Phe^{24}, and Lys^{25} amino acids in the Irga6 structure are shown.

ence of the nucleotide binding or C-terminal domains. Deletion of residues 2–12 or 7–12 had no effect on the *in vivo* expression of the 10D7 epitope in these short constructs, whereas the epitope was eliminated by deletion of residues 7–25 (data not shown). By a combination of site-directed mutagenesis and short deletions of the full-length protein, it was possible to locate the epitope definitively between residues 20 and 25. Full-length Irga6 proteins carrying single replacements of residues 20–25 with alanines were purified from *E. coli* extracts and probed with 10E7 and 10D7 in a Western blot (Fig. 6*A*). Side chains essential for the formation of the 10D7 epitope were found at Phe^{20} and Tyr^{23}; alanines at Gly^{22}, Phe^{24}, and Lys^{25} also weakened the signal. Alanine at Thr^{21} had no detectable effect, but a bulky substitution, T21I, also destroyed 10D7 binding (data not shown). Residues 20–25 of Irga6 make up most of Helix A (Fig. 6*B*), the first resolved helix of the Irga6 crystal structure (13). This α-helix is partly exposed to solvent in the structure and partly masked by contacts to Helix B, Helix C, and Helix F. Phe^{20}, Tyr^{23}, and Phe^{24} are buried in the interhelical space and not exposed on the solvent-accessible surface (Fig. 6*C*). In general, antibody epitopes on proteins are concentrated on loops and folds with a high degree of solvent exposure and are less common on regions of defined secondary structure (23, 24). Antibodies recognizing helical epitopes interact only with side chains on the exposed surface of the helix (25, 26). Taken together, therefore, the data suggest that the structure of the 10D7 epitope is not accurately reflected by Helix A of the crystal structure and that under conditions in which 10D7 binds to Irga6, Helix A is restructured into a solvent-exposed loop on which the linear epitope at residues 20–25 is accessible.

The expression of the 10D7 epitope in full-length Irga6 was further investigated by transfection of wild-type and certain mutant constructs into uninduced L929 fibroblasts followed by immunoprecipitation of Irga6 with 10D7 antibody in the presence and absence of GTPγS added to the detergent lysate and subsequent Western blot (Fig. 7). As predicted from the properties of 10D7 summarized above, immunoprecipitation of wild-type Irga6 from the lysate was absolutely dependent on the presence of GTPγS. The functionally dominant negative mutant Irga6-K82A, which can bind GTP with wild-type affinity but not hydrolyze it (19), and a second mutation, Irga6-

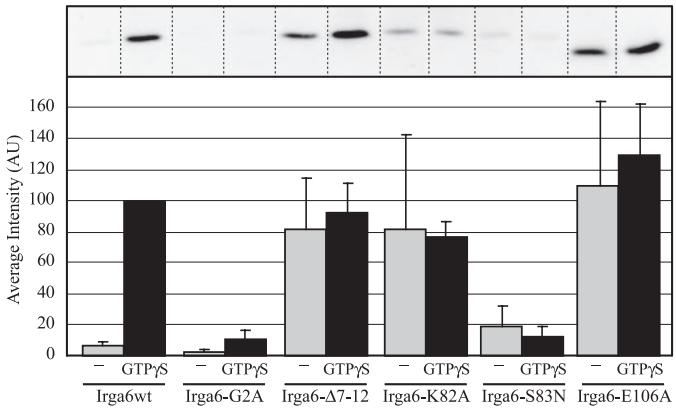

FIGURE 7. **10D7 antibody binds to the GTP-bound form of native cellular Irga6 but not to a myristoylation-deficient mutant.** L929 fibroblasts were transfected with Irga6wt, -G2A, -Δ7–12, -K82A, -S83N, or -E106A constructs. Cells were lysed 24 h later in Thesit in the absence or presence of 0.5 mM GTPγS, and Irga6 was immunoprecipitated with 10D7-Protein A-Sepharose beads. Irga6 proteins were detected in Western blot by rabbit anti-Irga6 polyclonal 165 serum. Signals were quantified using ImageQuant TLv2005, and values for immunoprecipitated proteins were normalized to the corresponding lysates. Mean values of at least three independent experiments are shown in the *histogram*. The 10D7 epitope is dependent on GTPγS in wild type Irga6 but constitutively expressed in functionally dominant negative mutants Irga6-K82A and -E106A. The myristoylation-deficient mutant, Irga6-G2A, cannot express the 10D7 epitope whether GTPγS is present or not. The mutant Irga6-Δ7–12 expresses 10D7 epitope independently of GTPγS.

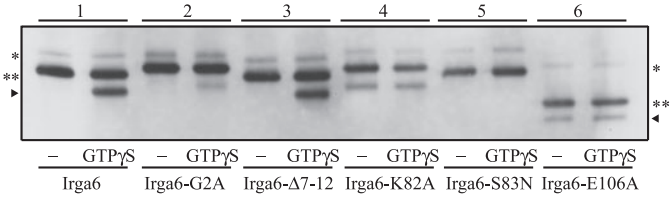

FIGURE 8. **The myristoyl group, but not the proximal part of Helix A, is important for GTP-dependent Irga6 self-interaction.** L929 fibroblasts were transfected with cTag1-tagged (**) and untagged (▶) wild type and mutant Irga6 constructs. The mutants Irga6-G2A, -Δ7–12, -K82A, -S83N, and -E106A were used. For each genotype, cells were transfected simultaneously with tagged and untagged constructs. Cells were lysed in Thesit 24 h later in the absence or presence of GTPγS and immunoprecipitated with anti-cTag1 serum. Irga6 proteins were identified with 10D7 antibody in Western blot. Only the Irga6wt and Irga6-Δ7–12 mutant showed typical GTPγS-dependent co-precipitation (*lanes 1* and *3*, respectively). The two functionally dominant negative mutants, Irga6-K82A and -E106A, both co-precipitated untagged protein independently of exogenous GTPγS (*lane 4* and *6*, respectively), whereas Irga6-G2A unexpectedly hardly co-precipitated untagged protein at all (*lanes 2*). Irga6cTag1-S83N showed no co-immunprecipitation of untagged protein (*lanes 5*). The *upper band* in each *lane*, labeled with a *single asterisk*, is the unexplained "transfection-specific" band referred to in the legend to Fig. 3.

E106A, which has similar properties,[6] were both immunoprecipitated by 10D7 whether GTPγS was added to the lysate or not, consistent with the expectation that these mutant proteins are already at least partially irreversibly GTP-bound at the time of lysis. Likewise, the nucleotide binding-deficient mutant Irga6-S83N (19) failed to bind significantly to 10D7 in absence or presence of GTPγS, consistent with the apparent GTP dependence of the epitope. Two mutants, however, failed to behave according to expectation in this assay. The mutant Irga6-Δ7–12 expressed the 10D7 epitope independently of GTPγS, whereas the mutant Irga6-G2A, which is mutated in the myristoyl attachment motif, failed to express the 10D7 epitope whether GTPγS was present or not. The behavior of these last two mutants suggested that expression of the 10D7 epitope is critically dependent on structural features at the N terminus that are not themselves part of the epitope and are also distant from the nucleotide binding site.

The apparently constitutive expression of the 10D7 epitope on the N-terminal deletion mutant, Irga6-Δ7–12, could suggest that this mutant, for unknown reasons, behaves like Irga6-K82A as a dominant negative, being constitutively GTP-bound in transfected cells. We investigated this possibility by co-immunoprecipitation from uninduced cells of transfected, untagged Irga6-Δ7–12 with transfected Irga6cTag1-Δ7–12. By this assay, Irga6cTag1-Δ7–12 (Fig. 8, *lanes 3*) behaved exactly like wild-type Irga6cTag1 (*lanes 1*), showing complete GTPγS dependence for co-precipitation of the untagged protein and thus suggesting that the nucleotide-binding site of this mutant is not irreversibly occupied by GTP. In contrast, in the same assay, the two functionally dominant negative mutants Irga6cTag1-K82A and Irga6cTag1-E106A (*lanes 4* and *6*, respectively) co-precipitated their untagged equivalents weakly but constitutively, independently of GTPγS, consistent with the expectation that these proteins were already partially in irreversible GTP-dependent aggregates before cell lysis, whereas the GTP binding-deficient mutant, Irga6cTag1-S83N (*lanes 5*), as expected, failed to co-immunoprecipitate the untagged mutant whether GTPγS was present or not. The myristoylation-deficient mutant, Irga6cTag1-G2A (*lanes 2*) showed very weak GTPγS-dependent co-precipitation of the untagged mutant, confirming that absence of the myristoyl group has seriously disturbed, if not completely destroyed, the normal conformational behavior of the mutant.

In aggregate, the data strongly suggest that complex conformational changes occur in Irga6 as a consequence of GTP binding. The 10D7 epitope is exposed by GTP binding although itself distant from the nucleotide binding site. Since the epitope is partially buried in the known crystal structures of Irga6 (13) and looks inaccessible to antibody, it is likely that GTP binding results in restructuring of the Helix A, exposing the whole linear epitope probably with partial unfolding. Indeed, the 10D7 epitope is probably loosely structured, since it is well expressed on Western blots of any Irga6 protein or fragment that contains the intact 20–25 sequence of Helix A. This property is also consistent with the fact that the 10D7 monoclonal antibody was produced in mice immunized with bacterially expressed Irga6 in Freund's complete adjuvant; the protein was probably largely denatured. In material isolated from cells, which is not intentionally denatured, the 10D7 epitope is constitutively exposed by loss of residues 7–12, which were not resolved in known crystal structures, suggesting that the presence of these residues is required to maintain Helix A in the "closed" configuration in the absence of GTP. Likewise, loss of the myristoyl moiety results in constitutive loss of the 10D7 epitope in material isolated from cells, hinting that a direct or indirect interaction between the myristoyl group and Helix A is required to enable the GTP-dependent conformational change in Helix A to occur in otherwise normally conformed molecules.

[6] N. Pawlowski, unpublished data.

DISCUSSION

In this study, we have provided evidence that Irga6 in interferon-induced cells must be predominantly GDP-bound (or possibly empty of nucleotide), whereas Irga6 that accumulates rapidly on the *T. gondii* parasitophorous vacuole in such cells is in the GTP-bound state. There are several grounds for believing that this change of state is accompanied by a significant conformational change in the Irga6 molecule. First, we present evidence that the target epitope of the anti-Irga6 monoclonal antibody, 10D7, is exposed on native wild-type Irga6 only when GTP, GTPγS, or GDP-AlFx is bound, and we show that it is strongly expressed on Irga6 associated with the *T. gondii* parasitophorous vacuole membrane (Fig. 1). Second, published *in vitro* experiments have shown that soluble monomeric Irga6 forms oligomers in the presence of GTP that can be stabilized by the presence of AlFx (16), showing that new interfaces are formed as a result of GTP binding and formation of the catalytic transition state that allow high affinity interaction between Irga6 monomers (Fig. 3). Finally, the binding of 10D7 to Irga6 molecules is influenced by at least two other elements of the protein for which unfortunately no structural information yet exists, namely amino acids 7–12 adjacent to the N terminus, which are not resolved in any crystal structure of Irga6 (13), and the myristoyl group, which was not present on the bacterially expressed protein from which the crystal structures were obtained. The individual absence of these two elements resulted in constitutive gain and constitutive loss, respectively, of the 10D7 epitope (Fig. 7).

On kinetic grounds, we should expect that cytoplasmic Irga6 will be predominantly in the GDP-bound form. The single-site equilibrium affinity constant of bacterially purified Irga6 for GDP is 15 times that for GTP (1 μM *versus* 15 μM) a difference accounted for entirely by the difference in off-rates (16), whereas the concentration of free cellular GTP is reported to be only 3-fold higher than that of GDP (330 μM *versus* 129 μM) (27). In addition, it is likely that the conformational change associated with GTP binding requires at least a dimerization of two GTP-bound Irga6 molecules (13), whereas the level of GTP-bound molecules will depend on the balance between the growth of GTP-bound, activated oligomers and their loss through hydrolysis of the bound GTP. Not all of the parameters required to calculate the expected level of GTP-bound, activated, oligomeric Irga6 are available, but it is clear that activated oligomers are expected to be rare relative to monomeric GDP-bound Irga6 or, presumably, nonactivated, monomeric Irga6 molecules, with GTP bound transiently to the low affinity binding site (16). Nevertheless, when Irga6 is expressed alone in uninduced cells, the protein accumulates in the GTP-bound state in aggregates of unknown structure (15, 19). We have shown that this transition is prevented in interferon-induced cells by direct interactions between Irga6 and three other members of the IRG family, the GMS proteins Irgm1, Irgm2, and Irgm3, with their distinctive G1 motif sequence in the nucleotide-binding site (19). In the case of Irgm3, we could also show that GDP is required for the interaction with Irga6 (19). Since the GMS proteins are predominantly or exclusively membrane-bound (15), we have argued that effective interactions between Irga6 and GMS proteins occur on cellular membranes rather than in the cytosol (19). Irga6 is ~60% bound to the ER membrane and 40% cytosolic in IFN-induced cells (15), presumably in a dynamic equilibrium, and it is plausible that the much higher effective concentration of Irga6 on ER membranes than in the cytosol tends to increase the rate of formation of activated GTP-bound dimers and oligomers in the transiently membrane-bound pool. Our speculation on the role of the GMS proteins is that they attenuate the activation process at intracellular membranes by retaining Irga6 molecules in the GDP-bound state until they are released from the membrane. In the absence of GMS proteins, in cells not stimulated with IFNγ and expressing Irga6 by transfection or by induction from a synthetic inducible promoter (19), activation of Irga6 proceeds until the rate of GTP hydrolysis is equal to the rate of growth of activated oligomers, resulting in a steady state with visible GTP-bound Irga6 accumulations with a high affinity for 10D7.

The role of the myristoyl group in the conformational transition associated with GTP-dependent activation of Irga6 and exposure of the 10D7 epitope is unclear. We have shown that the nonmyristoylated Irga6-G2A mutant can transfer only inefficiently to the parasitophorous vacuole in *T. gondii*-infected IFN-induced cells and also acts as a weak dominant negative, reducing the efficiency with which wild-type Irga6 accumulates on the vacuole.[7] This suggests that the myristoyl group is required for strong association of the activated protein with the PVM and is likely to be essential for the resistance function. A similar conjecture was made recently for the presumed myristoylation of another IRG protein, Irgb10, in its role in resistance of mouse cells against the vacuolar bacterium, *Chlamydia trachomatis* (28). Nevertheless, myristoylation cannot be a *sine qua non* of effector function in all IRG proteins, since several other members of the family do not carry a myristoylation signal, including all three GMS proteins as well as Irgb6 and Irgd (14). A GTP-dependent exposure of the myristoyl group associated with protein function at membranes is reminiscent of the properties of another myristoylated GTPase, ARF1, where the myristoyl group, normally partially buried in the protein structure, is exposed by a conformational change initiated by binding of GTP and contributes to the docking of ARF1 to its target membrane (29–31).

In Fig. 9*A*, we present a preliminary model for the conformational effects we have documented, based on the hypothesis that the 10D7 determinant is generated by a conformational transition in Helix A from a helical to an extended conformation, a transition that normally occurs when GTP-bound Irga6 monomers interact to form a dimer (or possibly higher order oligomer) and in which repositioning of the myristoyl group plays a role. We further hypothesize that such dimers or higher order oligomers, when assembled on the *T. gondii* PVM, represent the active form of the IRG protein, a form in which it is equipped to exercise its effector function against the parasite (Fig. 9*B*). By analogy with another large GTPase, dynamin, which associates with its target membranes

[7] N. Papic, unpublished data.

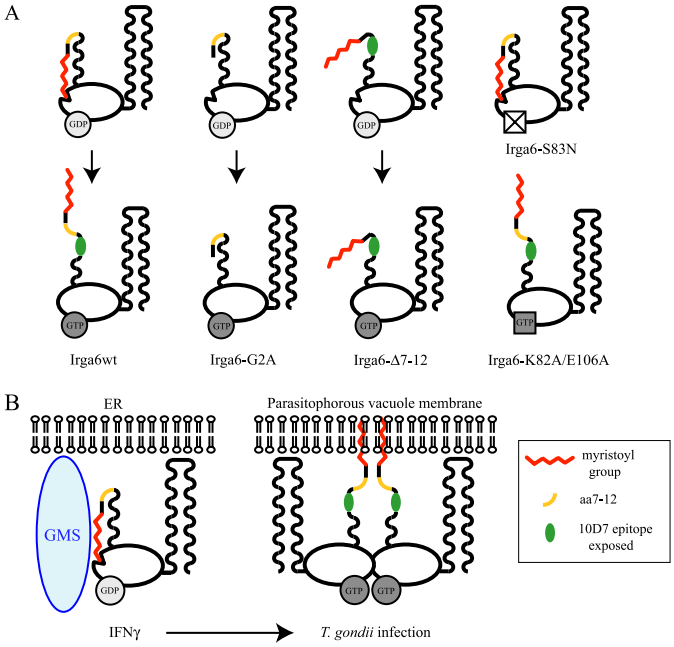

FIGURE 9. **Model of Irga6 nucleotide-dependent conformational change and membrane interaction.** *A*, the model proposes that regulated GTP binding by wild-type Irga6 initiates a complex conformational change requiring the presence of a "hinge" at residues 7–12 (*yellow strand*) that releases the myristoyl group (*red*) from a bound or cryptic configuration and exposes the 10D7 determinant by partial unfolding of Helix A residues 20–25 (*green oval*). In the absence of the myristoyl group (G2A), the motion is aborted for unknown reasons, and the 10D7 epitope is not exposed. In the Δ7–12 mutant, the critical hinge-like residues are absent, the myristoyl group is constitutively mispositioned, and the 10D7 epitope is constitutively exposed. In the S83N mutant, which cannot bind nucleotides, Irga6 is constitutively in the inactive, closed configuration, and the 10D7 determinant is constitutively not exposed. In the K82A and E106A mutants, Irga6 is constitutively GTP-bound *in vivo*, and the 10D7 determinant is constitutively exposed. *B*, in IFNγ-induced cells, the GMS group of 3 IRG proteins favor the GDP-bound inactive state of Irga6, which remains predominantly monomeric in the cytoplasm and at the ER membrane with the 10D7 epitope not exposed. Upon infection, Irga6 is released by an unknown mechanism from GMS control and interacts with the PVM in its GTP-bound form, probably by insertion of the myristoyl group, and exposing the 10D7 epitope. Homooligomerization of GTP-bound Irga6 could increase the avidity of this interaction, stabilizing active Irga6 on the vacuolar membrane.

at the neck of clathrin-coated endocytic invaginations in the GTP-bound state and functions in vesicle scission by hydrolysis of GTP (32, 33), it is plausible that the effector function of Irga6 and other IRG proteins of the GKS group is fulfilled via GTP hydrolysis at the parasitophorous vacuole membrane, leading to the observed vesiculation of the membrane (6, 8) and ultimately to its rupture.

Acknowledgments—We are grateful to Rita Lange, Manuel von Osten, and Claudia Poschner for assistance at various points during this study and to members of the laboratory for valuable discussions.

REFERENCES

1. Bernstein-Hanley, I., Coers, J., Balsara, Z. R., Taylor, G. A., Starnbach, M. N., and Dietrich, W. F. (2006) *Proc. Natl. Acad. Sci. U. S. A.* **103,** 14092–14097
2. Butcher, B. A., Greene, R. I., Henry, S. C., Annecharico, K. L., Weinberg, J. B., Denkers, E. Y., Sher, A., and Taylor, G. A. (2005) *Infect. Immun.* **73,** 3278–3286
3. Collazo, C. M., Yap, G. S., Sempowski, G. D., Lusby, K. C., Tessarollo, L., Woude, G. F., Sher, A., and Taylor, G. A. (2001) *J. Exp. Med.* **194,** 181–188
4. Feng, C. G., Collazo-Custodio, C. M., Eckhaus, M., Hieny, S., Belkaid, Y., Elkins, K., Jankovic, D., Taylor, G. A., and Sher, A. (2004) *J. Immunol.* **172,** 1163–1168
5. Halonen, S. K., Taylor, G. A., and Weiss, L. M. (2001) *Infect. Immun.* **69,** 5573–5576
6. Ling, Y. M., Shaw, M. H., Ayala, C., Coppens, I., Taylor, G. A., Ferguson, D. J., and Yap, G. S. (2006) *J. Exp. Med.* **203,** 2063–2071
7. MacMicking, J. D., Taylor, G. A., and McKinney, J. D. (2003) *Science* **302,** 654–659
8. Martens, S., Parvanova, I., Zerrahn, J., Griffiths, G., Schell, G., Reichmann, G., and Howard, J. C. (2005) *PLoS Pathog.* **1,** 187–201
9. Miyairi, I., Tatireddigari, V. R., Mahdi, O. S., Rose, L. A., Belland, R. J., Lu, L., Williams, R. W., and Byrne, G. I. (2007) *J. Immunol.* **179,** 1814–1824
10. Nelson, D. E., Virok, D. P., Wood, H., Roshick, C., Johnson, R. M., Whitmire, W. M., Crane, D. D., Steele-Mortimer, O., Kari, L., McClarty, G., and Caldwell, H. D. (2005) *Proc. Natl. Acad. Sci. U. S. A.* **102,** 10658–10663
11. Santiago, H. C., Feng, C. G., Bafica, A., Roffe, E., Arantes, R. M., Cheever, A., Taylor, G., Vieira, L. Q., Aliberti, J., Gazzinelli, R. T., and Sher, A. (2005) *J. Immunol.* **175,** 8165–8172
12. Taylor, G. A., Collazo, C. M., Yap, G. S., Nguyen, K., Gregorio, T. A., Taylor, L. S., Eagleson, B., Secrest, L., Southon, E. A., Reid, S. W., Tessarollo, L., Bray, M., McVicar, D. W., Komschlies, K. L., Young, H. A., Biron, C. A., Sher, A., and Vande Woude, G. F. (2000) *Proc. Natl. Acad. Sci. U. S. A.* **97,** 751–755
13. Ghosh, A., Uthaiah, R., Howard, J., Herrmann, C., and Wolf, E. (2004) *Mol. Cell* **15,** 727–739
14. Bekpen, C., Hunn, J. P., Rohde, C., Parvanova, I., Guethlein, L., Dunn, D. M., Glowalla, E., Leptin, M., and Howard, J. C. (2005) *Genome Biol.* **6, 92,** R1–R18
15. Martens, S., Sabel, K., Lange, R., Uthaiah, R., Wolf, E., and Howard, J. C. (2004) *J. Immunol.* **173,** 2594–2606
16. Uthaiah, R. C., Praefcke, G. J., Howard, J. C., and Herrmann, C. (2003) *J. Biol. Chem.* **278,** 29336–29343
17. Boehm, U., Guethlein, L., Klamp, T., Ozbek, K., Schaub, A., Futterer, A., Pfeffer, K., and Howard, J. C. (1998) *J. Immunol.* **161,** 6715–6723
18. Taylor, G. A., Stauber, R., Rulong, S., Hudson, E., Pei, V., Pavlakis, G. N., Resau, J. H., and Vande Woude, G. F. (1997) *J. Biol. Chem.* **272,** 10639–10645
19. Hunn, J. P., Koenen-Waisman, S., Papic, N., Schroeder, N., Pawlowski, N., Lange, R., Kaiser, F., Zerrahn, J., Martens, S., and Howard, J. C. (2008) *EMBO J.* **27,** 2495–2509
20. Gorini, G., Medgyesi, G. A., and Doria, G. (1969) *J. Immunol.* **103,** 1132–1142
21. Harlow, E., and Lane, D. (1988) *Antibodies: A Laboratory Manual*, pp. 516–523, Cold Spring Harbor Laboratory, Cold Spring Harbor, NY
22. Fazekas de St. Groth, S., Webster, R. G., and Datyner, A. (1963) *Biochim. Biophys. Acta* **71,** 377–391
23. Tainer, J. A., Getzoff, E. D., Paterson, Y., Olson, A. J., and Lerner, R. A. (1985) *Annu. Rev. Immunol.* **3,** 501–535
24. Thornton, J. M., Edwards, M. S., Taylor, W. R., and Barlow, D. J. (1986) *EMBO J.* **5,** 409–413
25. Lu, S. M., and Hodges, R. S. (2002) *J. Biol. Chem.* **277,** 23515–23524
26. Cardoso, R. M., Zwick, M. B., Stanfield, R. L., Kunert, R., Binley, J. M., Katinger, H., Burton, D. R., and Wilson, I. A. (2005) *Immunity* **22,** 163–173
27. Kleinecke, J., and Soeling, H. (1979) *FEBS Lett.* **107,** 1255–1265
28. Coers, J., Bernstein-Hanley, I., Grotsky, D., Parvanova, I., Howard, J. C., Taylor, G. A., Dietrich, W. F., and Starnbach, M. N. (2008) *J. Immunol.* **180,** 6237–6245
29. Goldberg, J. (1998) *Cell* **95,** 237–248
30. Gillingham, A. K., and Munro, S. (2007) *Annu. Rev. Cell Dev. Biol.*
31. Antonny, B., Beraud-Dufour, S., Chardin, P., and Chabre, M. (1997) *Biochemistry* **36,** 4675–4684
32. Tuma, P. L., and Collins, C. A. (1995) *J. Biol. Chem.* **270,** 26707–26714
33. Hinshaw, J. E., and Schmid, S. L. (1995) *Nature* **374,** 190–192